ELSEVIER

Thermochimica Acta 282/283 (1996) 251–264

thermochimica acta

Reduction of tungsten oxides with carbon. Part 1: Thermal analyses[1]

Dean S. Venables, Michael E. Brown*

Chemistry Department, Rhodes University, 6140 Grahamstown, South Africa

Abstract

The kinetics and mechanism of the reduction of WO_3 with carbon (in the form of graphite and of lamp black) were studied using isothermal thermogravimetry of small sample masses (< 50 mg) in the temperature range 935 to 1100°C. Two stages were observed in the reduction. The first stage corresponds approximately to the formation of WO_2 and the final product of the reduction was tungsten. The CO/CO_2 ratio in the gaseous products had a considerable influence on the reactions occurring.

The rate of the first stage of the reduction under isothermal conditions could be described by diffusion models, and is proposed to involve diffusion of CO(g) and CO_2(g) through the pores of the reacting tungsten oxides. The activation energies of the graphite and lamp black systems differed significantly for this first stage of reduction (386 compared to 465 kJ mol^{-1}). These activation energies are high for a diffusion process and may be inflated by changes in the structure of the product and the CO/CO_2 equilibrium ratio as the temperature increases. The rate of the second stage of reaction can be described by a first-order rate equation, and it is proposed that the second stage of reaction is limited by the reaction of carbon with carbon dioxide, rather than by the reduction of a tungsten oxide. The measured activation energy of 438 kJ mol^{-1} is slightly higher than the reported values for the carbon–carbon dioxide reaction (up to 400 kJ mol^{-1}).

Keywords: DTA; Diffusion mechanism; Graphite; Isothermal TG; Lamp black; Reduction of WO_3

* Corresponding author.

[1] Dedicated to Takeo Ozawa on the Occasion of his 65th Birthday.

SSDI 0040-6031(95)02814-6

1. Introduction

Tungsten carbide is produced by carburising tungsten powder with either methane or carbon in the presence of hydrogen gas [1]:

$$W \xrightarrow[>1400°C]{CH_4/C \quad H_2} WC$$

The properties of the resulting tungsten carbide powder are largely determined by the properties of the tungsten reactant. Consequently, a lot of work has concentrated on producing tungsten powder which is suitable for use in tungsten carbide production.

Growth of tungsten particles occurs during reduction in hydrogen, thus decreasing the value of the resulting tungsten powder. Water vapour produced by the reduction is responsible for the increase in particle size because it facilitates the transport of tungsten through the gas phase [2,3] via the formation of volatile $WO_2(OH)_2$ [4]. To minimise grain growth, small samples, low temperatures and high flowrates of hydrogen must be used. These conditions are costly to maintain and are not suited to large-scale industrial processing. Reduction using carbon alone is not usually employed because it introduces impurities and coarse tungsten particles are produced [1], although recent work by Asada et al. [5] has suggested that reduction with carbon may still be a viable process. Reduction of cobalt–tungsten oxides with hydrogen is reported [6] to be improved in the presence of solid carbon. On thermodynamic grounds, carbon is likely to reduce the concentration of water vapour in the system, which could improve the properties of the resulting tungsten and tungsten carbide powders.

This paper deals with the kinetics of reduction of tungsten oxides by carbon, determined from thermal analyses. In the second part [7], reactions of larger samples in a tube furnace system are described. In further papers, the reduction by hydrogen alone, and simultaneously by hydrogen and carbon [8] are reported. Reduction by carbon monoxide was also studied [9] since this is a likely intermediate in the reaction involving carbon.

2. Experimental

2.1. Materials

WO_3 (98% pure, Saarchem) was sieved to give a 53–75 μm mesh fraction. Scanning electron microscopy showed cube-like particles.

Graphite and lamp black (both 99% pure, Saarchem) were used as the source of carbon. The graphite was < 53 μm mesh. Particles had jagged, irregular shapes. The lamp black consisted of very small particles which formed fluffy agglomerates.

WO_2 was prepared by reducing WO_3 at 800°C under hydrogen which had been bubbled through water. $W_{18}O_{49}$ was prepared in a similar manner at 700°C.

High purity argon and hydrogen were supplied by Fedgas. Both gases contained less than 3.0 vpm O_2 and 2.0 vpm H_2O.

Weighed samples of tungsten oxides and graphite or lamp black were mixed in a three-dimensional motion mixture for 18 h.

2.2. Thermal Analysis

A Perkin-Elmer TGA-7 system was used below 900°C. Loose powder samples (5 to 40 mg) were contained in platinum pans. The temperature of the TG furnace was calibrated with the Curie points of nickel (354°C) and iron (780°C). Experiments at higher temperatures were carried out on a Setaram TGA 92 system. Samples of 40 to 90 mg were heated in an alumina crucible in an argon atmosphere.

A Perkin–Elmer DTA 1700 system was used for differential thermal analysis (DTA) experiments. Sample masses of between 10 and 60 mg were heated in an alumina crucible in argon.

2.3. Other techniques

The size and morphology of the reactant and product powders were studied using a JEOL JSM-840 scanning electron microscope. The size distributions of WO_3, graphite, and lamp black powders were determined by laser diffraction in a Malvern Instruments MasterSizer at AECI Ltd. A Phillips X-ray diffractometer was used to record the powder diffraction patterns of the sample at various stages of the reduction.

3. Results

3.1. Thermogravimetry of WO_3–graphite mixtures

The TG curve of a 1:3 mole ratio mixture of WO_3 and graphite heated in argon at 2°C min^{-1} up to 950°C (not illustrated) showed that the mass decreases very slowly from 750 to 900°C, and starts decreasing more rapidly above 900°C. A DTA curve of the same mixture up to 1200°C showed a shallow endotherm from about 930 to 1110°C. Reaction between WO_3 and graphite is thus only significant above 900°C and may take place in two stages.

Only a limited number of isothermal TG experiments could be done, due to limited time available on the instrument and the considerable wear-and-tear on the instrument under the experimental conditions required.

Mixtures of WO_3 and graphite in a 1:3 mole ratio were studied at 950, 1050, and 1100°C. The isothermal mass loss curves are shown in Fig. 1 and indicate that the course of reaction changes markedly with temperature. At 950°C, the TG curve is smooth and the reaction is about a third complete after about 4 h. The mid-temperature range (1050°C) shows overlapping processes, which are less evident at higher temperatures (1100°C). The transition between the first and second stages

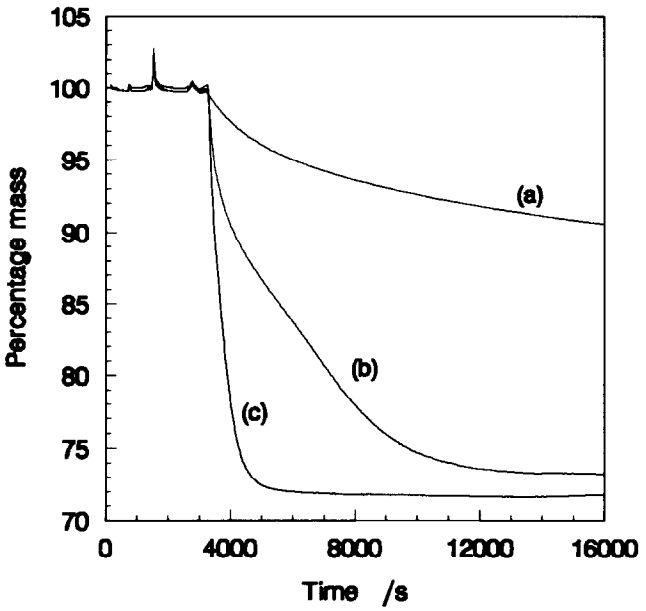

Fig. 1. Isothermal TG curves for mixtures of WO_3 and graphite in a 1:3 mole ratio heated in argon at (a) 950, (b) 1050, and (c) 1100°C.

occurs between 8 and 13% mass loss, suggesting a two-stage reduction:

$$WO_3 \rightarrow WO_2 \quad (1)$$

followed by

$$WO_2 \rightarrow W \quad (2)$$

The mass losses of these steps (as a percentage of the original WO_3–graphite mixture) vary from 8.2 to 10.5% for the first stage, and 16.4 to 20.9% for the second stage, depending on the relative amounts of CO and CO_2 formed in the reaction. Thus, the total mass loss for complete reaction ranges from 24.6 to 31.4%.

3.2. Thermogravimetry of WO_3–lamp black mixtures

The isothermal TG curves obtained at 950°C using graphite and using lamp black were similar (Fig. 2). Increasing the temperature to 1000°C gave no indication of a two-stage process.

3.3 Kinetic analysis

3.3.1. Isothermal experiments

3.3.1.1. WO_3–graphite The kinetics of the first and second stages of the reaction were analysed separately. The reaction rate was deceleratory over the entire course of the

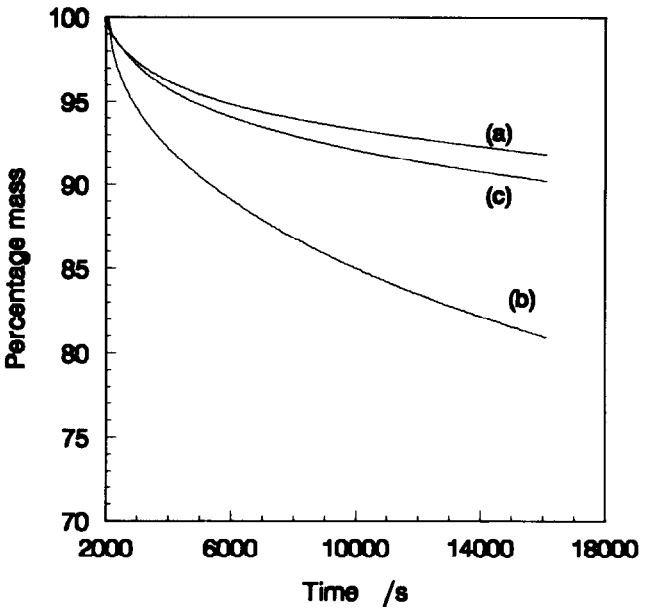

Fig. 2. Isothermal TG curves obtained in argon: (a) WO_3–lamp black at 950°C; (b) WO_3–lamp black at 1000°C; (c) WO_3–graphite at 950°C.

reaction. The extent of reaction based on the completion of the first stage (taken as 10.5%) is designated as α', whereas α indicates the extent of the overall reaction. At 950 and 1050°C the reaction was taken to be complete at 26.9% (the final mass loss at 1050°C), and at 1100°C the reaction was assumed complete at 28.4%, the final mass loss at that temperature. Only the rate coefficients determined from α values were used for activation energy calculations.

Kinetic analysis of the isothermal α'–time curve at 950°C, showed that the Ginstling–Brounshtein (D4) and one-dimensional diffusion (D1) models [10] gave the best fit to the experimental data (Fig. 3). The R2, R3, and F1 models did not fit the data well.

The rate constants obtained over the range $0 < \alpha < 0.29$ are shown in Table 1.

At 1050°C the D4 model gave the best fit to the initial part of the curve ($\alpha < 0.60$), and at higher α values the F1 model fitted the curve well ($0.78 < \alpha < 0.97$). The applicability of the D4 model extended over a larger range of α than that expected if the reduction of WO_3 to WO_2 constituted the first stage ($0.26 < \alpha < 0.33$). The D4 model also fitted the α' values well, so it is not clear whether the diffusion-limiting process applies to complete reduction, or only the reduction to WO_2. The calculated rate coefficients are $(234.9 \pm 2.9) \times 10^{-7} s^{-1}$ for the D4 model, and $(560 \pm 2) \times 10^{-6} s^{-1}$ for the F1 model. Using these values, and taking the start of applicability of the models at $t = c/k$ (where c is the intercept and k is the rate coefficient calculated in the linear regression), the experimental α–t curve may be compared with the curves calculated using the D4 and F1 models (Fig. 4). The transition from the D4 to the F1 model occurs at about $\alpha = 0.67$.

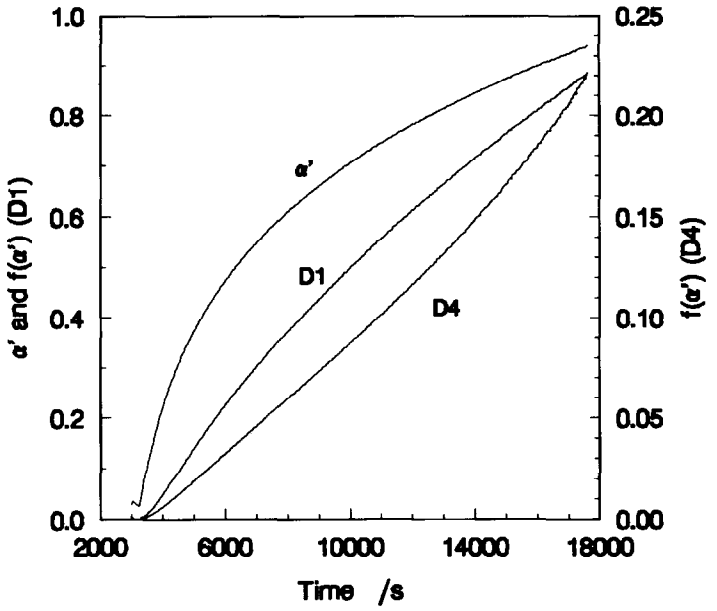

Fig. 3. Kinetic analysis of the isothermal α' against time curve at 950°C in terms of the Ginstling-Brounshtein (D4) and one-dimensional diffusion (D1) models.

Table 1
The rate constants and correlation coefficients calculated using the D1 and D4 models for the WO_3–graphite system at 950°C for $\alpha < 0.29$

	D1/(10^{-6} s^{-1})	r^2	D4/(10^{-6} s^{-1})	r^2
k'	61.3 ± 0.3	0.9885	15.0 ± 0.1	0.9942
k	11.1 ± 0.1	0.9950	1.43 ± 0.01	0.9974

The rate coefficients calculated using the D3 and D4 models for the WO_3–lamp black system at 950°C

Rate coefficient	D3/(10^{-7} s^{-1})	D4/(10^{-7} s^{-1})
k'	110 ± 1	80.1 ± 0.1
k	6.22 ± 0.03	6.99 ± 0.03

At 1100°C the first stage of the reaction was completed too rapidly ($\alpha < 0.40$) for reliable comparison of kinetic models. A D4 model was assumed on the basis of the results at 950 and 1050°C, and gave $k = (9.25 \pm 0.57) \times 10^{-5}$ s^{-1} for $\alpha < 0.40$. For the second stage of the reaction, the F1 model gave the best fit to the data. For $0.65 < \alpha < 0.95$ the value of k was $(239 \pm 1) \times 10^{-5}$ s^{-1}. The transition between models takes place at about $\alpha = 0.47$.

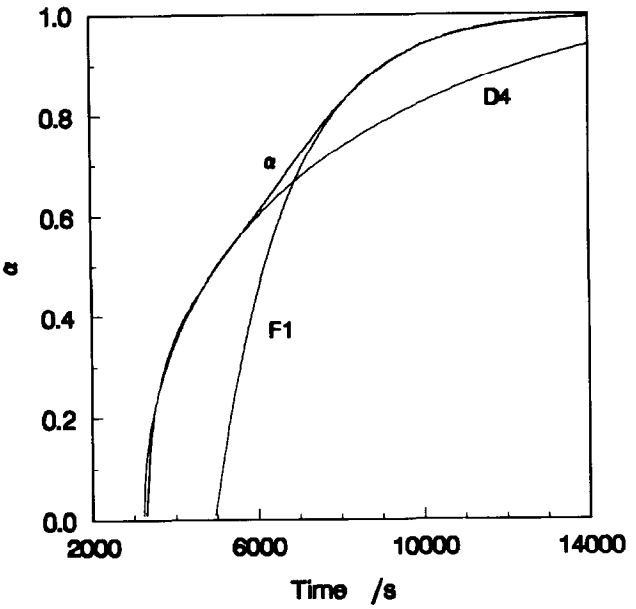

Fig. 4. Comparison of the experimental α, t curve at 950°C with the curves calculated using the D4 and F1 models.

The k values calculated using the D4 and F1 models were incorporated in an Arrhenius plot. The values calculated for the activation energy and the frequency factor were 386 ± 9 kJ mol^{-1} and $(4.36 \pm 0.3) \times 10^{10}$ s^{-1} for the D4 model, and 438 kJ mol^{-1} and 1.13×10^{14} s^{-1} for the F1 model.

The small number of experimental curves obviously decreases the certainty of the results.

3.3.1.2. WO_3–lamp black At 950°C, the diffusion models showed good fits using the values of α'. The fit of the D4 model was best. The calculated rate coefficients are listed in Table 1. The diffusion models also gave good agreement with the experimental α values at 1000°C.

An activation energy of 465 kJ mol^{-1} and a frequency factor of 5.21×10^{13} s^{-1} were calculated using the D4 model.

3.3.2. Dynamic experiments

The kinetics of the reactions were examined using the Borchardt and Daniels method [11], where rate coefficients, k, are calculated from $k = (d\alpha/dt)(1 - \alpha)^{-n}$, where n is the "order of the reaction", and these k values are used in an Arrhenius plot. The values of n considered were 0.333, 0.5, 0.667, 1, 1.5, and 2. A seven-point cubic Savitzky–Golay [12] smoothing routine was used to smooth the data and compute the first derivative for the analysis.

The method of Gyulai and Greenhow [13] was used to analyse the data from experiments carried out at different heating rates. This method does not assume a particular form for $f(\alpha)$.

A Borchardt and Daniels plot of $\ln k$ against $1/T$ is shown in Fig. 5. The plot is approximately linear over two sections. The first section occurred from about 915 to 1050°C, followed by a steeper slope from 1050 to 1125°C. The transition region at about 1050°C corresponds to $\alpha = 0.27$, which is quite close to $\alpha = 0.33$, the transition point expected for a two step process proceeding via reduction of the dioxide. Higher orders of reaction fitted the data best for temperatures below 1050°C, whereas from 1050 to 1125°C the lower orders give the best fit (Table 2).

Similar results were obtained for an experiment at 10°C min^{-1} and are included in Table 2. A reaction order of 2 gave the best fit at low temperatures, and above 1058°C orders of 1 and 1.5 gave the closest fit.

The Gyulai-Greenhow method was applied to the results from experiments at heating rates of 5 and 10°C min^{-1}. The α values chosen for the analysis were 0.05, 0.10, and 0.20 for the first stage of the reduction, and 0.40, 0.50, and 0.60 for the second stage. Fig. 6 shows the plot for the first stage. An activation energy of between 300 and 360 kJ mol^{-1} was calculated. The activation energy for the second stage of the reduction varied considerably with the value of α and was also very high (well above 600 kJ mol^{-1}).

For the reduction of WO_3 with lamp black, the reaction mixture was heated at 5°C min^{-1} and the results were analysed in the same manner as above. The Borchardt and

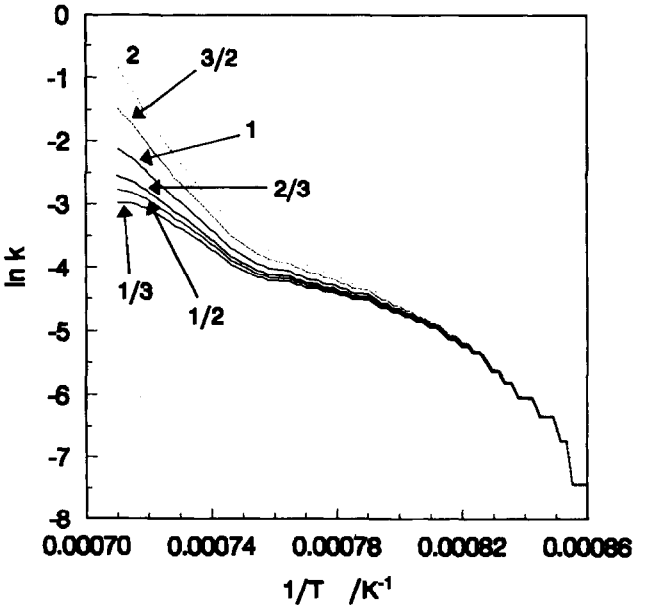

Fig. 5. A Borchardt and Daniels plot for different orders of reaction for WO_3–graphite, heated at 5°C min^{-1}, $k = (d\alpha/dt)/(1-\alpha)^{-n}$ in units of min^{-1}.

Table 2
The calculated activation energies for different orders of reaction for WO_3–graphite, heated at 5°C min^{-1}.

n	915 to 1050°C		1050 to 1125°C	
	E_a/(kJ mol^{-1})	r^2	E_a/(kJ mol^{-1})	r^2
0.333	174 ± 7	0.9281	255 ± 3	0.9953
0.5	179 ± 7	0.9343	279 ± 3	0.9970
0.667	184 ± 7	0.9401	304 ± 3	0.9973
1.0	194 ± 7	0.9501	352 ± 4	0.9960
1.5	208 ± 6	0.9621	424 ± 8	0.9919
2.0	222 ± 6	0.9713	496 ± 11	0.9874

The calculated activation energies for different orders of reaction for WO_3–graphite, heated at 10°C min^{-1}

n	932 to 1058°C		1058 to 1121°C	
	E_a/(kJ mol^{-1})	r^2	E_a/(kJ mol^{-1})	r^2
0.333	194 ± 8	0.9421	313 ± 10	0.9826
0.5	199 ± 8	0.9468	337 ± 9	0.9875
0.667	203 ± 8	0.9511	361 ± 8	0.9908
1.0	213 ± 7	0.9588	408 ± 7	0.9943
1.5	226 ± 7	0.9681	479 ± 8	0.9951
2.0	240 ± 6	0.9754	549 ± 10	0.9836

The calculated activation energies for different orders of reaction for WO_3–lamp black mixtures, heated at 5°C min^{-1}

n	900 to 1040°C		1040 to 1140°C	
	E_a/(kJ mol^{-1})	r^2	E_a/(kJ mol^{-1})	r^2
0.333	152 ± 2	0.9892	184 ± 2	0.9973
0.5	155 ± 2	0.9906	203 ± 2	0.9976
0.667	159 ± 2	0.9919	223 ± 2	0.9969
1.0	165 ± 2	0.9940	262 ± 4	0.9939
1.5	175 ± 2	0.9962	321 ± 6	0.9884
2.0	186 ± 1	0.9975	380 ± 9	0.9833

Daniels plot also formed two parts. The transition temperature was at about 1040°C, at which α was about 0.30. The results are included in Table 2. As for the WO_3–graphite mixtures, a reaction order of 2 fitted the data best at lower temperatures; low reaction orders fitted the data well at higher temperatures. The activation energies calculated for the lamp black system were significantly lower than for the graphite system.

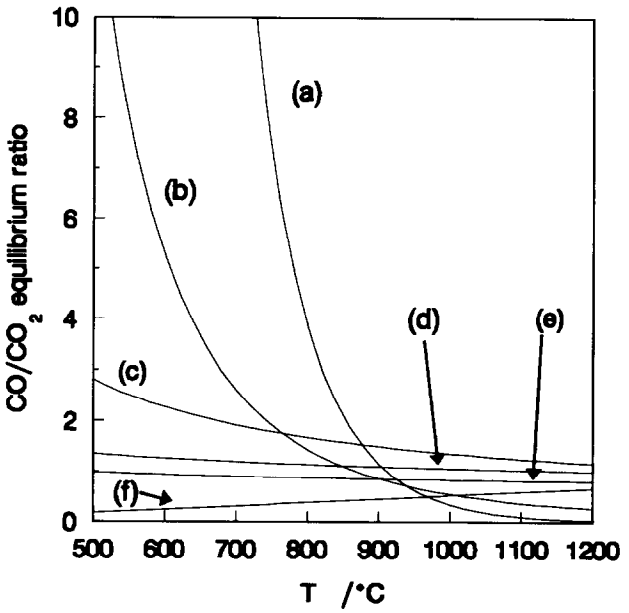

Fig. 6. The equilibrium ratios for the reactions: (a) $W + 2CO \rightarrow WC + CO_2$; (b) $WO_2 + 4CO \rightarrow W + 3CO_2$; (c) $WO_2 + 2CO \rightarrow W + 2CO_2$; (d) $W_{18}O_{49} + 49CO \rightarrow 18W + 49CO_2$; (e) $W_{18}O_{49} + 85CO \rightarrow 18WC + 67CO_2$; (f) $W_{18}O_{49} + 13CO \rightarrow 18WO_2 + 13CO_2$.

4. Discussion

In isothermal experiments, two distinct stages were observed in the reduction at 1050°C and 1100°C, with the transition between stages occurring between $0.2 < \alpha < 0.4$. Dynamic experiments also showed a transition in the kinetics of the reduction occurring at about 1040 to 1060°C, corresponding to α between 0.25 to 0.30. These results are consistent with a two-stage reduction of WO_3. WO_2 seems to be the most likely intermediate on the basis of the mass losses, although the formation of $W_{20}O_{58}$ and $W_{18}O_{49}$ may also be inferred from the results for the reduction with CO [9] and from the morphology of the products.

The D4 (Ginstling-Brounshtein) model gave the closest fit to the first stage of the reduction in isothermal experiments. The diffusion which this equation models may either be that of gases through the pores of the solid or diffusion of species through the crystal lattice. In the present study, the reaction must be limited by pore diffusion because, as shown by electron microscopy, the structure of the reactant particles changes from non-porous WO_3 to a more porous structure of $W_{18}O_{49}$ and WO_2. Thus, a reacting WO_3 particle will have a non-porous core of WO_3 or $W_{20}O_{58}$ surrounded by a porous layer of product, probably WO_2 and $W_{18}O_{49}$. CO and CO_2 would be able to diffuse much more rapidly through the pores in the particle than by diffusion through the crystal structure of the product. Access to the reaction interface by CO or to the surface of the particle by CO_2 would be relatively easy. Consequently, any diffusion through the crystal lattice which contributed to the reaction process

would only occur at a receding reaction interface. Such a mechanism would be described by the contracting-area or contracting-volume models (i.e., R2 and R3), and not by a diffusion model.

The D4 model could therefore describe diffusion of CO and CO_2 through the pores of the reacting tungsten oxides. The activation energy calculated for the first stage would then correspond to the activation energy for pore diffusion and not for the reaction between WO_3 and CO. The kinetic parameters of the actual chemical reaction could then only be determined indirectly, by studying the reaction of WO_3 with CO separately, at temperatures at which the chemical reaction is much slower than pore diffusion.

Because the first stage of the process is limited by pore diffusion, the differences in the rates of reaction of WO_3 with graphite and with lamp black are probably caused by different CO/CO_2 ratios in these systems. At 950°C, the lamp black is not as reactive as graphite towards CO_2. Considering that the temperature is the same and that the CO/CO_2 ratios in the systems are unlikely to differ substantially, it seems improbable that the different reaction rates are caused by dissimilarities in the structures of the reacting tungsten oxide particles. Since the source of carbon does not affect the CO/CO_2 equilibrium ratio [14], the CO/CO_2 ratios in the system must be significantly below the equilibrium concentration in at least some of the experiments.

The activation energies determined for the first step are therefore related to the reactivities of graphite and lamp black towards CO_2 but are unlikely to be directly related to reaction (3).

$$C(s) + CO_2(g) \rightarrow 2CO(g) \quad (3)$$

Lamp black is less reactive towards CO_2 than graphite at low temperatures, but the higher activation energy for the lamp black system implies a higher temperature-dependence of the reaction than the graphite system. Using the kinetic parameters determined above, the rate of the first stage of reaction of WO_3 with lamp black should exceed that with graphite above 1070°C. Variations in the reactivities of different forms of carbon are well documented [15].

The second stage of reaction can be described by a first-order rate equation. Reaction (3) is known to be first-order [15–17] which suggests that the second stage of reaction is also limited by reaction (3), and not by the reduction of a tungsten oxide. Indeed, it is difficult to conceive a process whereby the reduction depends solely on the amount of tungsten oxide. Such a reaction mechanism implies that CO has access to all the tungsten oxide (both the surface and the bulk) over the duration of the second stage. It does appear that such is the case, but the observation is only superficially correct because the tiny particles comprising the pseudomorph are themselves non-porous. In effect, the reaction still takes place between CO and non-porous particles, and reaction must start at the external surface of these particles.

If the second stage of the reaction is limited by the rate of reaction (3), then the relative rates of the first and second stages seem anomalous. For if reaction (3) limits the rate of the second stage of the process, then it should also be rate-limiting for the first stage of the reaction because the second stage of reaction occurs more slowly than the first stage.

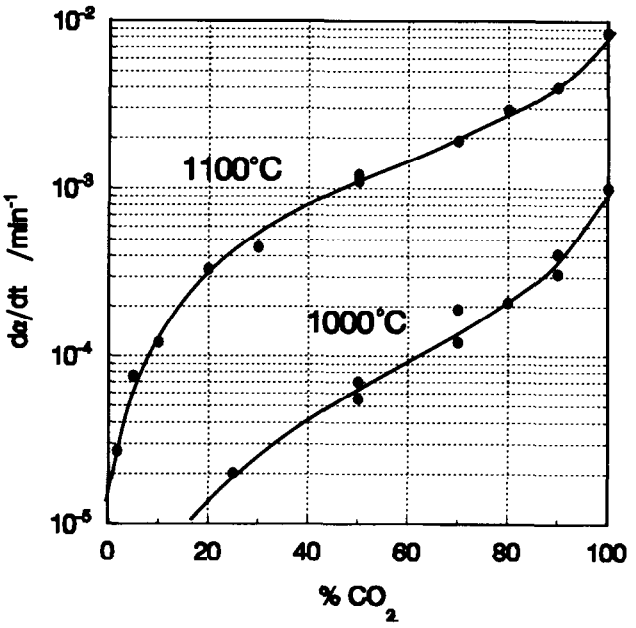

Fig. 7. The effect of temperature and gas composition on the rate of the reaction C(s) + CO_2(g) → 2CO(g) in CO_2–CO mixtures [13].

The difficulty can be resolved by considering the effect of the CO/CO_2 ratio on the reduction of WO_3 and WO_2. The rate of reaction of CO_2 with C must be known as a function of the CO/CO_2 ratio. Referring to Fig. 6, it is clear that the CO content in the gas phase must be much higher to reduce WO_2 to tungsten than to reduce WO_3 to WO_2. For instance, at 1000°C the concentration of CO must be above 58% by volume to reduce WO_2 (if the remainder of the gas is CO_2), whereas to reduce WO_3 to WO_2 requires a CO/CO_2 ratio above 0.19 (that is, at least 16% CO by volume in CO_2).

The rate equation for reaction (3) is [14]:

$$\text{rate} = k_1 p(CO_2)/\{1 + k_2 p(CO) + k_3 p(CO_2)\}$$

and indicates that the rate of reaction depends strongly on the CO/CO_2 ratio. This dependence is shown in Fig. 7, which is from the work of Turkdogan and Vinters [5]. Using the above example, at 1000°C the rate of reaction at a CO/CO_2 ratio of 0.19 is about three times higher than at a CO/CO_2 ratio of 1.37. The rate of reaction (3) will also decrease as carbon is used up during the reaction. These general considerations explain how the rate may be limited by different processes during the reduction.

Although the activation energies of the graphite and lamp black systems differed significantly for the first stage of reduction (386 compared to 465 kJ mol^{-1}), the systems were examined at different temperatures. These activation energies are high for a diffusion process, and may be inflated by changes in the structure of the product and

the CO/CO_2 equilibrium ratio as the temperature increases. The structure of the product is more open at higher temperatures, which would facilitate the diffusion of gases in the tungsten oxide and thus increase the rate constant for the reaction. The higher CO/CO_2 ratio in the powder layer might also result in a significant increase in the rate of reduction.

The first-order reaction model, Fl, described the second stage of the reaction and gave an activation energy of 438 kJ mol^{-1}. This activation energy is slightly higher than the reported values for reaction (3), which range up to 400 kJ mol^{-1}. Considering the complexity of the system and that only two points were used to calculate the activation energy, this discrepancy is not significant.

As is often found, the results obtained from the dynamic experiments were less consistent than the isothermal results. A second-order rate equation fitted the data best at low temperatures and gave an activation energy of between 220 and 240 kJ mol^{-1} for the graphite system, compared to 186 kJ mol^{-1} for the lamp black system. Above the transition temperature, reaction orders between 0.5 and 1.5 fitted the data well. Changing the reaction order made little difference to the fit of the equation but altered the value of the activation energy considerably. Thus, the activation energies calculated for $n = 0.5$ to 1.5 varied between 300 and 480 kJ mol^{-1}. The activation energy for the reaction using lamp black was considerably lower, between 180 and 225 kJ mol^{-1} for reaction orders of 0.333 to 0.667. Better results from the dynamic experiments were obtained using the Gyulai-Greenhow approach. For the first stage of the reduction the activation energy was between 300 and 360 kJ mol^{-1}, which compares favourably with the isothermal results.

Acknowledgements

The authors acknowledge with gratitude the advice and assistance given by Karol Cameron, Ian Sutherland and Ian Porée of the Solid State Chemistry Group, AECI Chemicals Ltd, and financial support from AECI Chemicals Ltd and the Foundation for Research Development.

References

[1] J.A. Mullendore, in *Kirk-Othmer Encyclopedia of Chemical Technology*, 3rd edn., Vol. 23, John Wiley and Sons, New York, 1983, pp. 413ff.
[2] W.D. Schubert and E. Lassner, Int. J. Ref. Hard Met., 10 (1991) 171.
[3] W.D. Schubert and E. Lassner, Int. J. Ref. Hard Met., 10 (1991) 133.
[4] T. Millner and J. Neugebauer, Nature (London), 163 (1949) 601.
[5] N. Asada, Y. Yamamoto, K. Shimatani, S. Honkawa and M. Miyake, *Hardmetal Ostem, Japan*, April 15–26, 5.9.1–5.9.28.
[6] A.S. Petukhov, L.D. Konchakovskaya, I.V. Uvarova and L.G. Reiter, Poroshk. Metall. (Kiev), (6) (1990) 33 (Chem. Abstr., 114 (1991) 10482v).
[7] D.S. Venables and M.E. Brown, Thermochim. Acta, accepted for publication.
[8] D.S. Venables and M.E. Brown, Thermochim. Acta, accepted for publication.
[9] D.S. Venables and M.E. Brown, Thermochim. Acta, accepted for publication.

[10] M.E. Brown, D. Dollimore and A.K. Galwey, *Comprehensive Chemical Kinetics: Reactions in the Solid State*, Vol. 22, C.H. Bamford and C.F.H. Tipper (Eds.), Elsevier, Amsterdam, 1980.
[11] H.J. Borchardt and F. Daniels, J. Am. Chem. Soc., 79 (1957) 41.
[12] A. Savitzky and M.J.E. Golay, Anal. Chem., 36 (1964) 1627.
[13] G. Gyulai and E.J. Greenhow, Thermochim. Acta, 6 (1973) 239.
[14] P.L. Walker, F. Rusinko and L.G. Austin, in *Adv. Catal.*, Vol. 11, D.D. Eley, P.W. Selwood and P.B. Weisz (Eds.), Academic Press, New York, 1959.
[15] E.T. Turkdogan and J.V. Vinters, Carbon, 8 (1970) 39.
[16] Y.K. Rao, Metall. Trans., 2 (1971) 1439.
[17] A.K. Basu and F.R. Sale, Metall. Trans., 9B (1978) 603.